LASER INTERFEROMETER GRAVITATIONAL WAVE OBSERVATORY

LIGO Laboratory / LIGO Scientific Collaboration

LIGO- **T1100056**-v1 *LIGO* 1/13/11

Arm Cavity Baffle Edge Scatter

Michael Smith

Distribution of this document:
LIGO Scientific Collaboration

This is an internal working note
of the LIGO Laboratory.

California Institute of Technology
LIGO Project – MS 18-34
1200 E. California Blvd.
Pasadena, CA 91125
Phone (626) 395-2129
Fax (626) 304-9834
E-mail: info@ligo.caltech.edu

Massachusetts Institute of Technology
LIGO Project – NW22-295
185 Albany St
Cambridge, MA 02139
Phone (617) 253-4824
Fax (617) 253-7014
E-mail: info@ligo.mit.edu

LIGO Hanford Observatory
P.O. Box 159
Richland WA 99352
Phone 509-372-8106
Fax 509-372-8137

LIGO Livingston Observatory
P.O. Box 940
Livingston, LA 70754
Phone 225-686-3100
Fax 225-686-7189

http://www.ligo.caltech.edu/

Table of Figures

Abstract

The scatter from the exposed frontal edges of the Arm Cavity Baffle is calculated. It depends upon the BRDF characteristics of the baffle material at small angles, upon the vertical tilt angle of the baffle edge, and upon the radius of the edge.

1 Introduction

This document presents a calculation of the light scattered into the IFO arm cavity mode by the exposed vertical edges of the Arm Cavity Baffle.

The scatter from the exposed frontal edges of the Arm Cavity Baffle depends upon the BRDF characteristics of the baffle material at small angles, upon the vertical tilt angle of the baffle edge, and upon the radius of the edge.

2 Scattering Theory

The primary source of scattered light from the Arm Cavity Baffle (ACB) is the small angle scatter from the COC mirror at the far end of the arm tube. This light will scatter from the edges and the bends of the ACB as shown in Figure 3 and Figure 4.

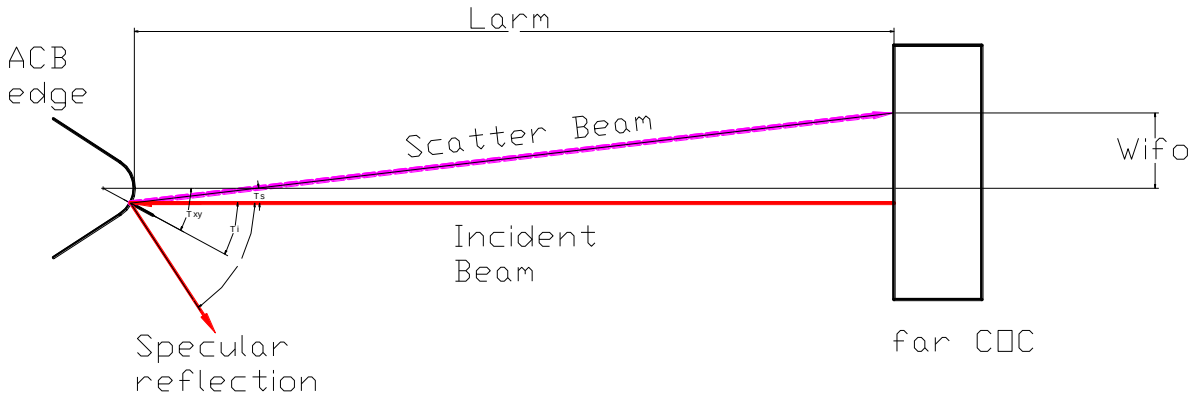

Figure 1:Light from the far mirror scatters from the ACB edge back into the IFO mode

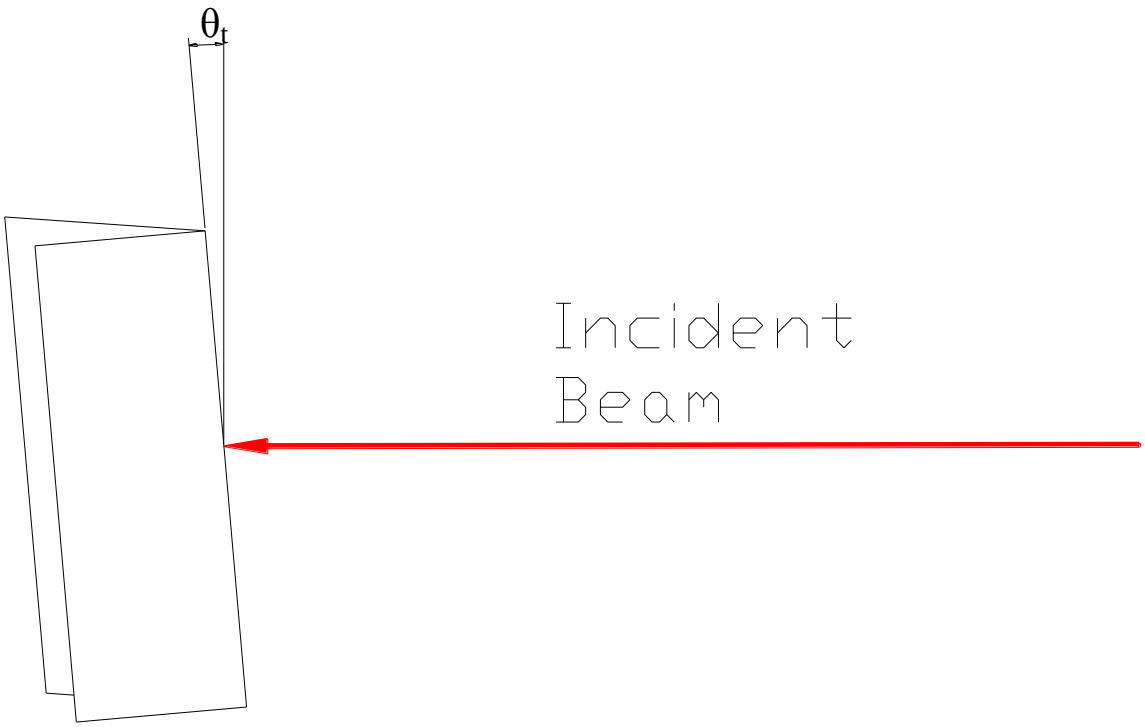

Figure 2: ACB is tilted to reduce the back scatter

The incident angle at the baffle surface is θ_i , which depends upon θ_{xy} , the angle of the normal to the surface,l and θ_t , the tilt angle.

$$\theta_i(\theta_t, \theta_{xy}) := \operatorname{acos}\left(\cos(\theta_{xy})\cdot\cos(\theta_t)\right)$$

The light must scatter by the angle $2\theta_i \pm \theta_s$ in order to back-scatter into the incident beam direction.

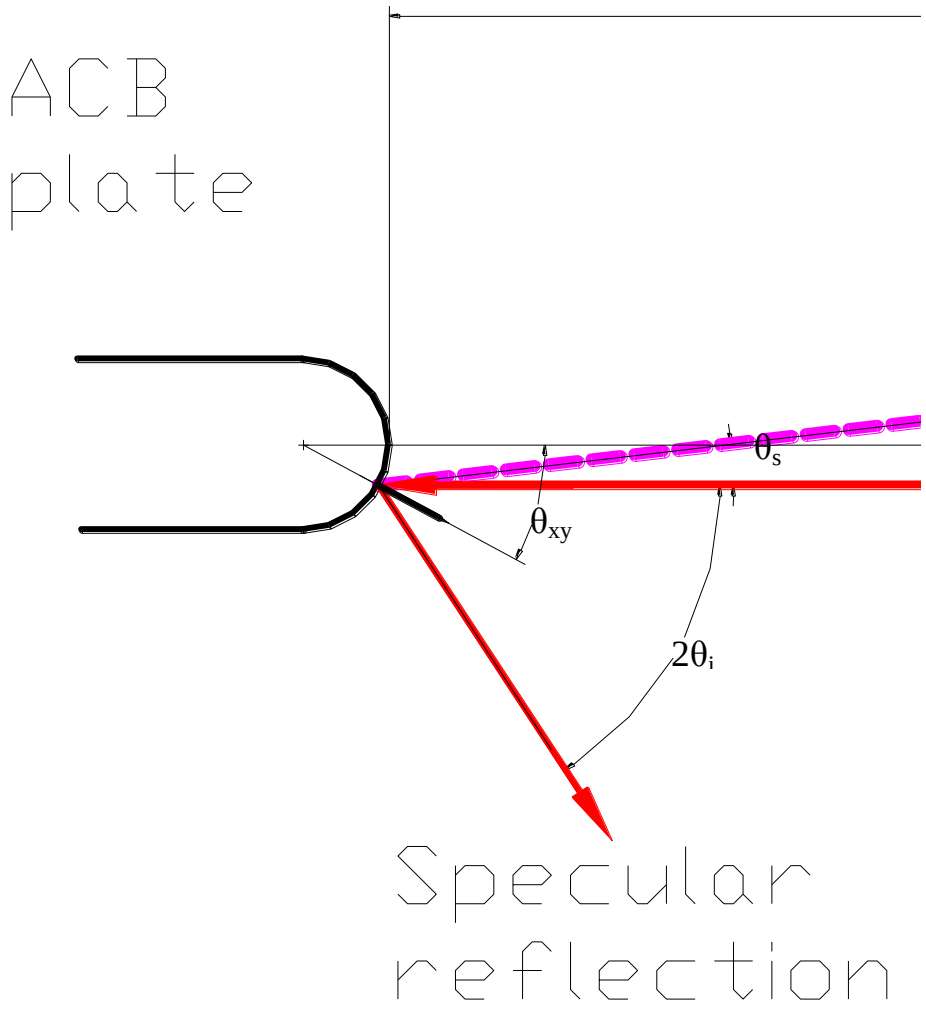

Figure 3: Geometry of the scattering calculation for the baffle plate edge

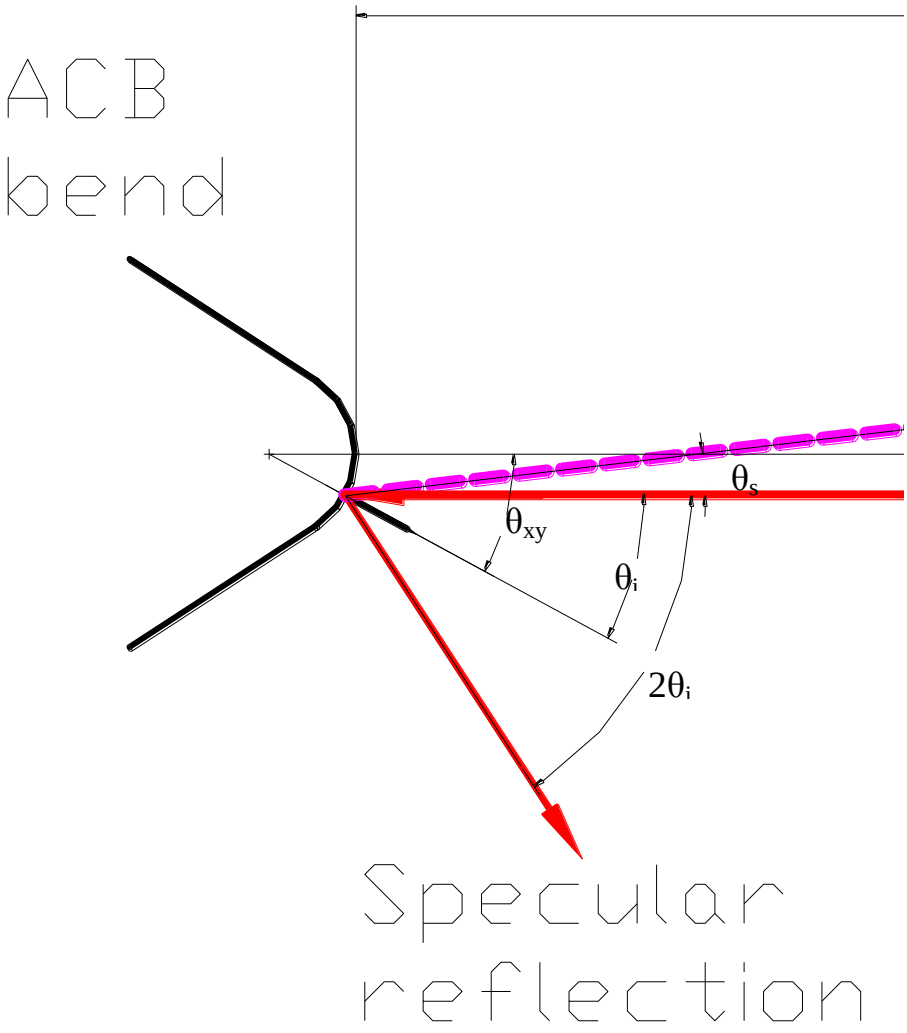

Figure 4: Geometry of the scattering calculation for the baffle bend

2.1 Parametric BRDF Function

The angular dependence of the BRDF of the ACB surface with respect to the incidence angle can be approximated by the following parametric expression. The parameters are adjusted to match the shape of the BRDF data as measured by the CASI scatterometer.

$$BRDF_{ACB}(\theta_i) := \frac{BRDF_0}{\left(1 + C_{mr}\cdot\theta_i^{\,2}\right)^{\beta}} + BRDF_{\theta 2}$$

The estimated maximum value at normal incidence is $BRDF_0$. The break-over angle, θ_1 is the angle at which the $BRDF_0$ value is half the maximum. The BRDF reaches a minimum constant value, $BRDF_{\theta 2}$, for angles greater than the micro-roughness angle, θ_2.

The slope modifier, β is chosen to match the slope of the measured BRDF function.

The micro-roughness constant, C_{mr} is chosen so that the BRDF is equal to the minimum value at large scattering angles.

micro-roughness constant $$C_{mr} := \frac{2^{\frac{1}{(\beta)}} - 1}{\theta_1^{\,2}}$$

2.2 Scattered Power into IFO

The light back-scattered into the interferometer mode from the incident beam power, $dP_i(\theta_{xy})$ at an incident angle on the baffle surface θ_i is centered around the scatter angle $2\theta_i$. This light is scattered into the solid angle subtended by the area of the IFO mode divided by the (arm length)^2, and must be re-scattered by the surface of the COC mirror at the far end of the arm to enter the divergence cone of the IFO.

$$dP_{sIFO} = dP_i(\theta_{xy})\, BRDF_{ACB}(2\theta_i + \theta_s)\,(dA_{IFO}/L_{arm}^{\,2})\, BRDF_{COC}\, \Delta\Omega_{IFO}$$

The incident power is equal to the incident radiant intensity, I_i, times the element of ACB scattering area.

$$dP_i(\theta_{xy}) = I_i\, r H \sin(\theta_{xy})\, d\theta_{xy}$$

where r is the radius of the baffle edge and H is the vertical height of the baffle edge.

The element of area of the IFO mode into which the light scatters is given by

$$dA_{IFO} = 2[w_{IFO}^{\,2} - (L_{arm}\,\theta_s)^2]^{1/2}$$

where w_{IFO} is the radius of the IFO mode.

The total power back-scattered into the IFO mode is calculated by integrating over the scattering angle and over all incident angles at the ACB scattering surface.

$$P_{acbedgepsifo}(\theta_t, r) := 4 \cdot I_i \cdot r \cdot H_p \cdot BRDF_1\left(30 \cdot 10^{-6}\right) \cdot \Delta\Omega_{ifo} \cdot \left(S_p(\theta_t)\right)$$

The integrated scattering function is given by.

$$S_p(\theta_t) := \int_0^{\theta_{xymaxp}} \left[\int_{2\cdot\theta_i(\theta_t,\theta_{xy})-\frac{w_{ifo}}{L_{arm}}}^{2\cdot\theta_i(\theta_t,\theta_{xy})+\frac{w_{ifo}}{L_{arm}}} BRDF_{ACBporc}\left(\theta_s + 2\cdot\theta_i(\theta_t,\theta_{xy})\right)\cdot\sqrt{w_{ifo}^2 - \left[L_{arm}\cdot\left(\theta_s - 2\cdot\theta_i(\theta_t,\theta_{xy})\right)\right]^2}\cdot\frac{L_{arm}}{L_{arm}^2}\, d\theta_s \right] \cdot\cos\left(\theta_{xy}\right) d\theta_{xy}$$

The maximum incident angles for the bent baffle edge and for the plate edge are given below.

input angle range, bend, rad $\theta_{xymaxb} := 33 \cdot \frac{\pi}{180} = 0.576$

input angle range, plate rad $\theta_{xymaxp} := \frac{\pi}{2} = 1.571$

The Baffle and IFO parameters used for the calculations are given below.

length of baffle plate edge, m $H_p := 0.65$

length of baffle bend edge, m $H_b := 2 \cdot 0.239 = 0.478$

laser wavelength, m $\lambda := 1.064 10^{-6}$

IFO waist size, m $w_{ifo} := 0.01$

solid angle of IFO mode, sr $\Delta\Omega_{ifo} := \frac{\lambda^2}{\pi \cdot w_{ifo}^2} = 2.502 \times 10^{-9}$

Transfer function @ 100 Hz, ITM HR $TF_{itmhr} := 1.1 \cdot 10^{-9}$

IFO arm length, m $L_{arm} := 400$

Arm Power, W $P_0 := 83417$

radius of Cryopump aperture, m $R_{cp} := 0.384$

half-angle from centerline to Rcp, rad $\theta_{cp} := \frac{R_{cp}}{L_{arm}}$

The scattering characteristics of the COC mirror is modeled with the following parametric function.

BRDF, sr^-1; CSIRO, surface 2, S/N 2

$$BRDF_1(\theta) := \frac{2755.12}{\left(1 + 8.5078710^{8}\cdot\theta^{2}\right)^{1.23597}}$$

3 Results

3.1 Measured BRDF

The BRDF of porcelainized steel and oxidized polished stainless steel was measured with the CASI scatterometer. The scatterometer has a blind spot and cannot measure the maximum BRDF at the specular angle; therefore, the maximum BRDF and the break-over angle must be estimated by achieving the best fit of the data with the parametric equation. In the following, two sets of scatterometer data from different positions on the same sample, together with the instrument background signal and the best-fit parametric equation are shown. BRDF values are valid above the level of the instrument background signal, shown in the red trace.

3.1.1 Porcelainized Steel @ 3 Degree Incidence Angle

The CASI BRDF data for two positions on a porcelainized steel sample @ 3 deg incidence is shown in Figure 5.

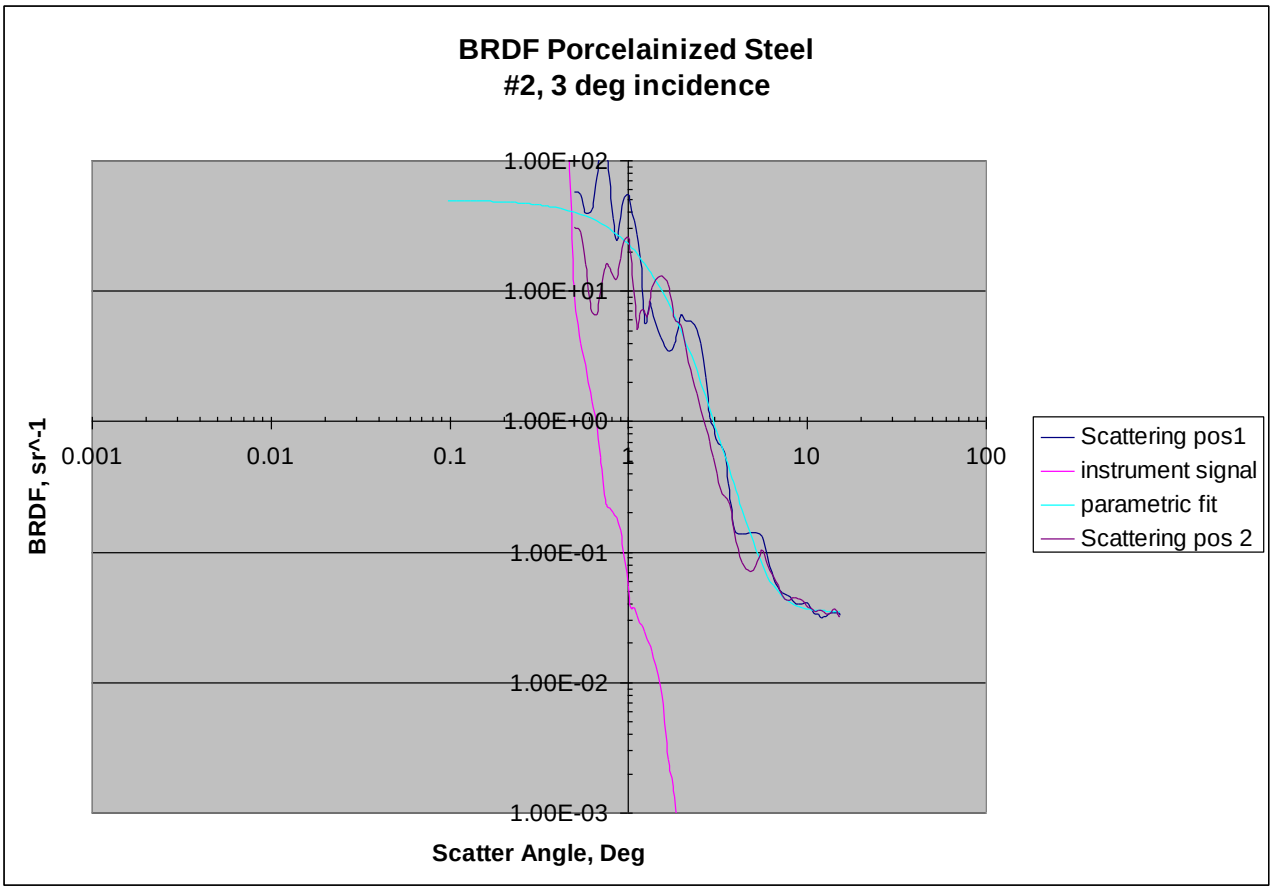

Figure 5: CASI Measurement of BRDF of Porcelainized Steel @ 3 Deg Incidence

Reflectivity of surface @ 3 deg incidence	R = 0.02
Break-over angle	θ_1 = 0.9 deg
Micro roughness angle	θ_2 = 6 deg
Maximum $BRDF_0$	$BRDF_0$ = 50
Slope modifier	β =2.7
Micro-roughness constant	C_{mr} = 1186

The parametric equation with the best-fit to the scattering data is plotted in Figure 6.

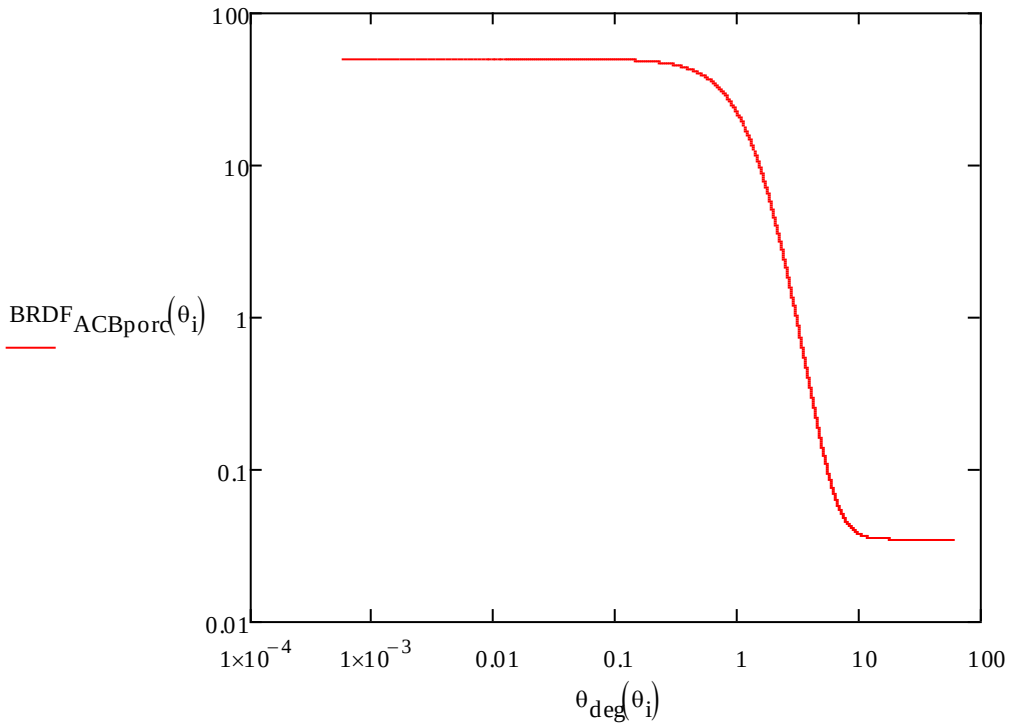

Figure 6: Parametric Equation, Porcelainized Steel BRDF Versus Scattering Angle Around the Specular Direction

3.1.2 Oxidized Polished Stainless Steel @ 3 Degree Incidence Angle

The CASI BRDF data for two positions on an oxidized polished stainless steel with four passes through the oxidizing furnace is shown in Figure 7.

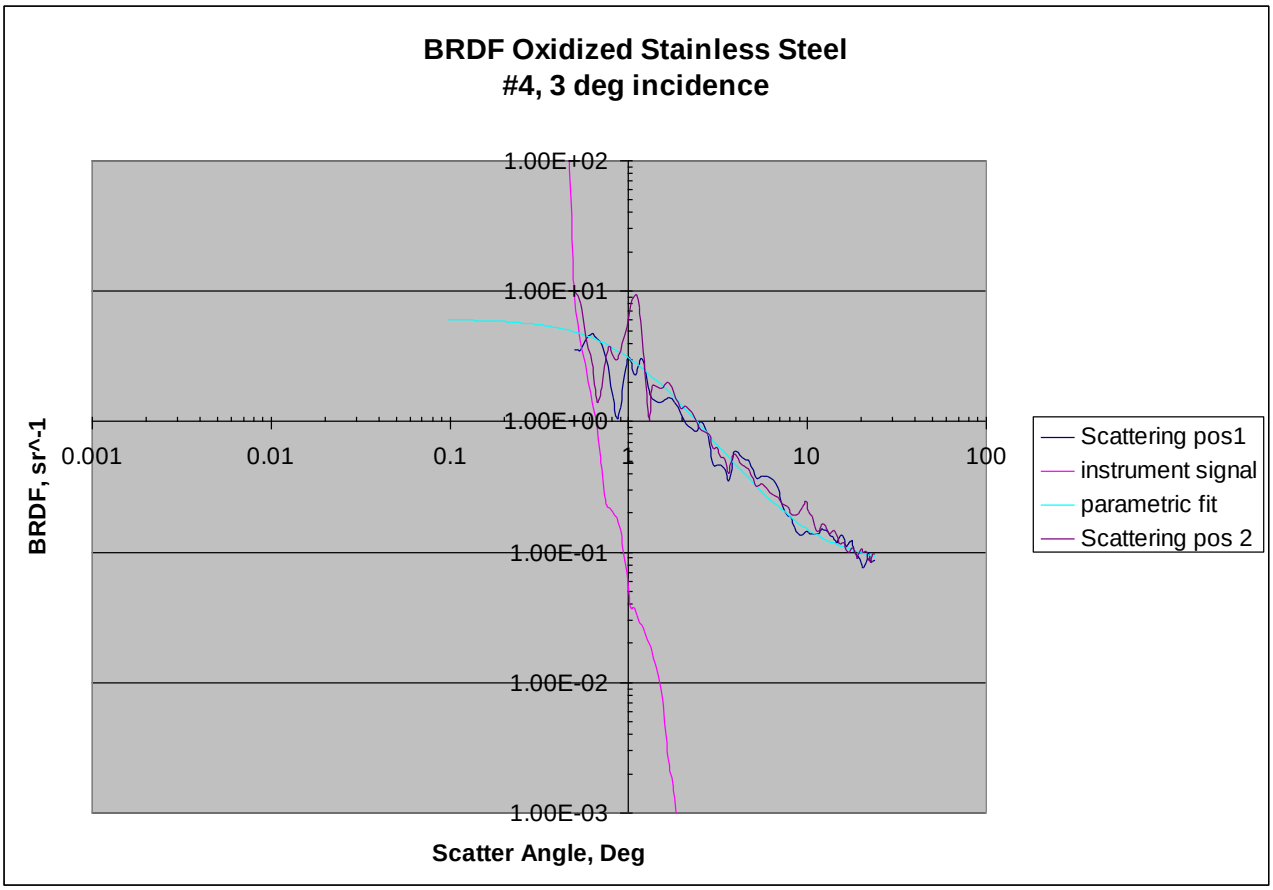

Figure 7: CASI Measurement of BRDF of #4 Oxidized Polished Stainless Steel @ 3 Deg Incidence

Reflectivity of surface @ 3 deg incidence	R = 0.02
Break-over angle	θ_1 = 1 deg
Micro roughness angle	θ_2 = 10 deg
Maximum $BRDF_0$	$BRDF_0$ = 6
Slope modifier	β = 0.95
Micro-roughness constant	C_{mr} = 3527

The parametric equation with the best-fit to the scattering data is plotted in Figure 8.

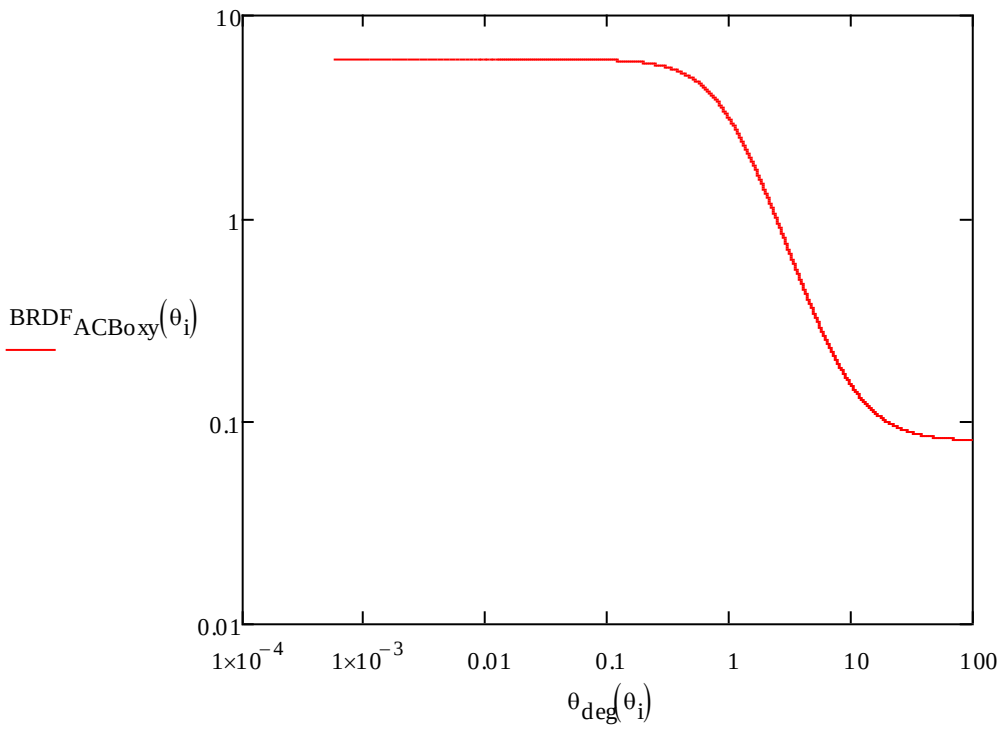

Figure 8: Parametric Equation, #4 Oxidized Polished Stainless Steel @ 3 Deg Incidence BRDF Versus Scattering Angle Around the Specular Direction

A comparison of the BRDFs for porcelainizing and oxidizing is shown in Figure 9.

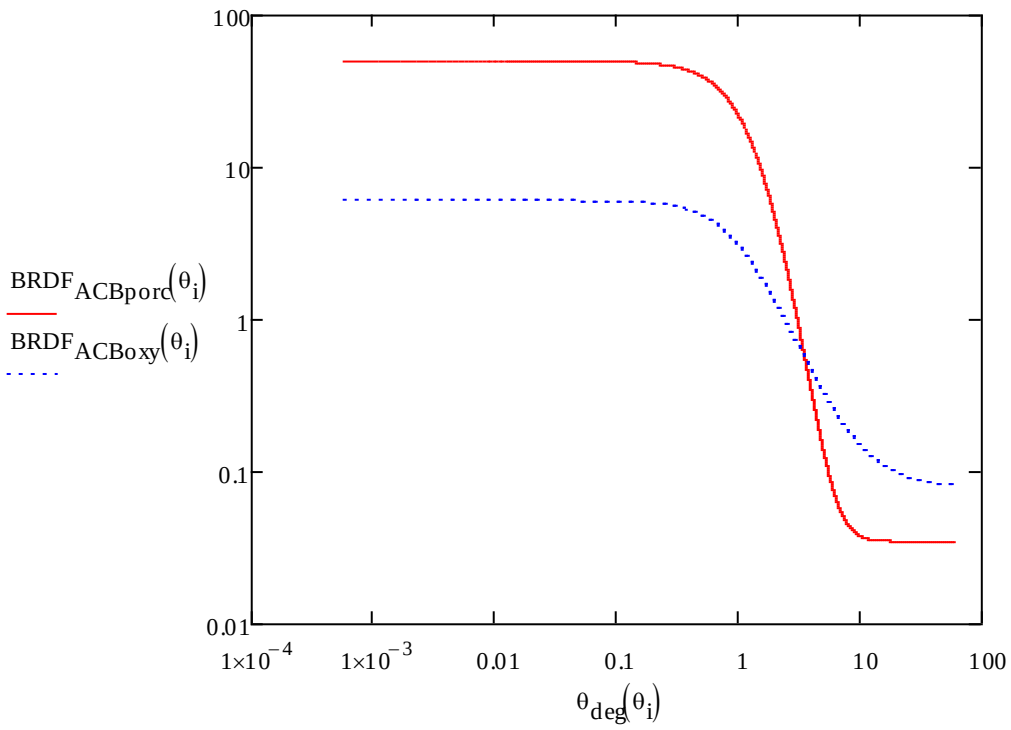

Figure 9: Comparison of #4 Oxidized Polished SS and Porcelainized steel @ 3 Deg Incidence

3.2 Scattered Light Calculations

3.2.1 Baffle Irradiance

power through the cryopump baffle aperture (hits the arm cavity baffle), W

$$P_{acb} := P_a \cdot \int_0^{\theta_{cp}} 2\cdot\pi\cdot\theta\cdot BRDF_1(\theta)\, d\theta$$

$$P_{acb} = 14.573$$

Area of cryopump baf aperture, m^2

$$A_{cp} := \pi \cdot R_{cp}^{\ 2} = 0.464$$

incident intensity, W/m^2

$$I_i := \frac{P_{acb}}{A_{cp}} = 31.376$$

3.2.2 Power Scattered into IFO Mode from Baffle Plate Edge

The scattered light from the ACB edge, as a function of tilt angle for edge radii 1, 2, and 4 mm, is shown in Figure 10.

$$P_{acbporcedgepsifo}(\theta_t, r) := 4 \cdot I_i \cdot r \cdot H_p \cdot BRDF_1\left(30 \cdot 10^{-6}\right) \cdot \Delta\Omega_{ifo} \cdot \left(S_p(\theta_t)\right)$$

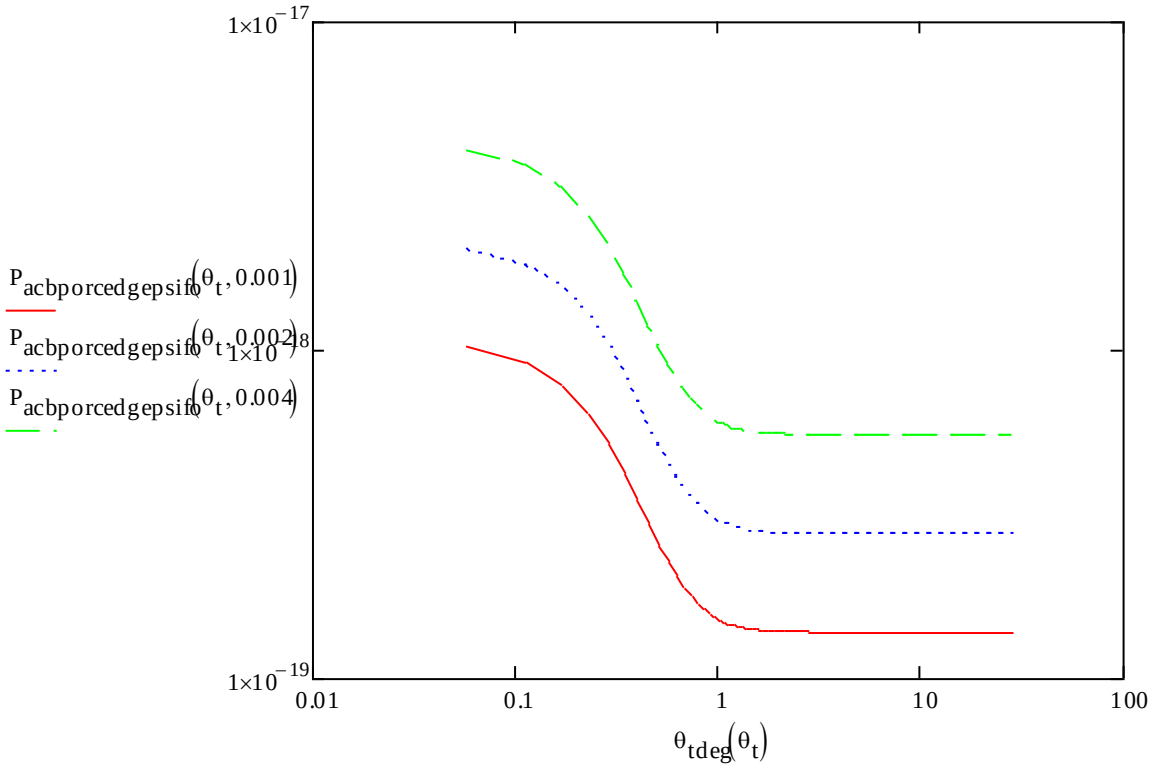

Figure 10: Power Scattered into the IFO Mode from the Baffle Plate Edge, Porcelainized Steel

3.2.3 Power Scattered into IFO Mode from Baffle Plate Bend

The scattered light from the ACB bend as a function of tilt angle for edge radii 1, 2, and 4 mm is shown in Figure 11.

$$P_{acbporcedgebsifo}(\theta_t, r) := 4 \cdot I_i \cdot r \cdot H_b \cdot BRDF_1\left(30 \cdot 10^{-6}\right) \cdot \Delta\Omega_{ifo} \cdot \left(S_p(\theta_t)\right)$$

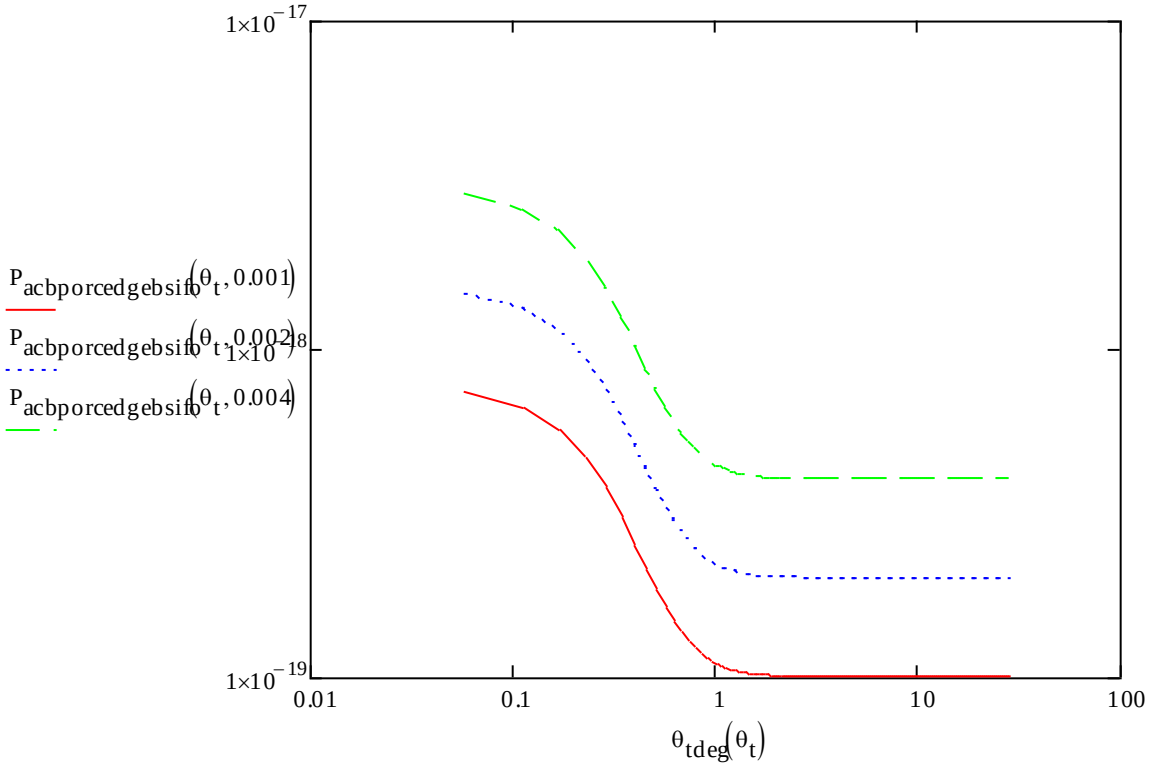

Figure 11: Power Scattered into the IFO Mode from the ACB Bend, Porcelainized Steel

Note that minimum scattering occurs when the baffle is tilted to approximately 1 deg, for this particular BRDF function.

3.2.4 Total Power Scattered into IFO Mode from Baffle Plate Edge, Bend, and the Louver Surfaces of the ACB

The louver surfaces of the ACB are inclined at an incidence angle of 57 deg. The frontal area of the louver surfaces is

$$A_{ACB} = 0.236 \text{ m}\hat{}2$$

The power into the IFO mode by the louver surface is given by

$$P_{acbporcsifo} := I_i \cdot A_{ACB} \cdot BRDF_{ACBporc}\left(2 \cdot 57 \cdot \frac{\pi}{180}\right) \cdot \frac{w_{ifo}^2}{L_{arm}^2} \cdot BRDF_1\left(30 \cdot 10^{-6}\right) \cdot \Delta\Omega_{ifo}$$

The BRDF of porcelainized steel at the incident angle of the louver plates is

$$BRDF_{ACBporc}\left(2 \cdot 57 \cdot \frac{\pi}{180}\right) = 0.035$$

The total scattered power by all parts of the ACB is given by

$$P_{acbtsifo}(\theta_t, r) := P_{acbedgepsifo}(\theta_t, r) + P_{acbedgebsifo}(\theta_t, r) + P_{acbsifo}$$

3.2.5 Displacement Noise Due to Total ACB Scatter

3.2.5.1 Porcelainized Steel Scatter Noise

The displacement noise @ 100 Hz due to the ACB scatter, as a function of tilt angle, is shown in

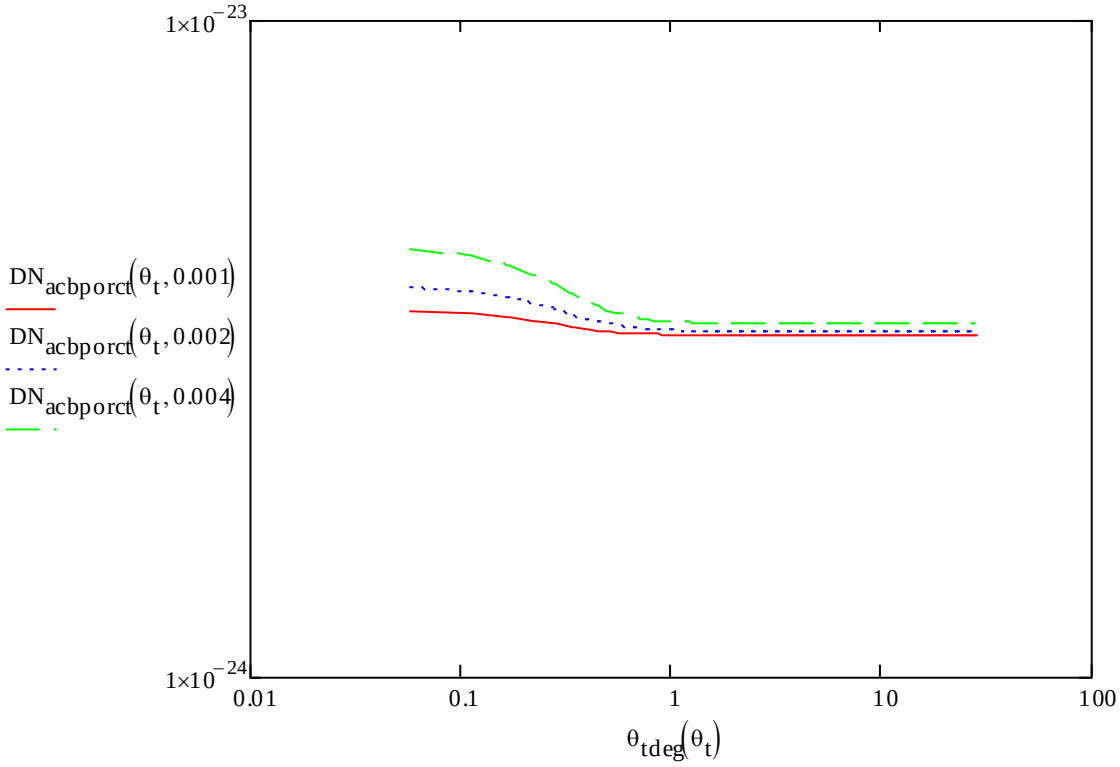

Figure 12.

ACB displacement @ 100 HZ, m/rt HZ $x_{ACB} := 1 \cdot 10^{-12}$

$$DN_{acbporct}(\theta_t, r) := TF_{itmhr} \cdot \left(\frac{P_{acbporctsifo}(\theta_t, r)}{P_{psl}} \right)^{0.5} \cdot x_{ACB} \cdot 2 \cdot k$$

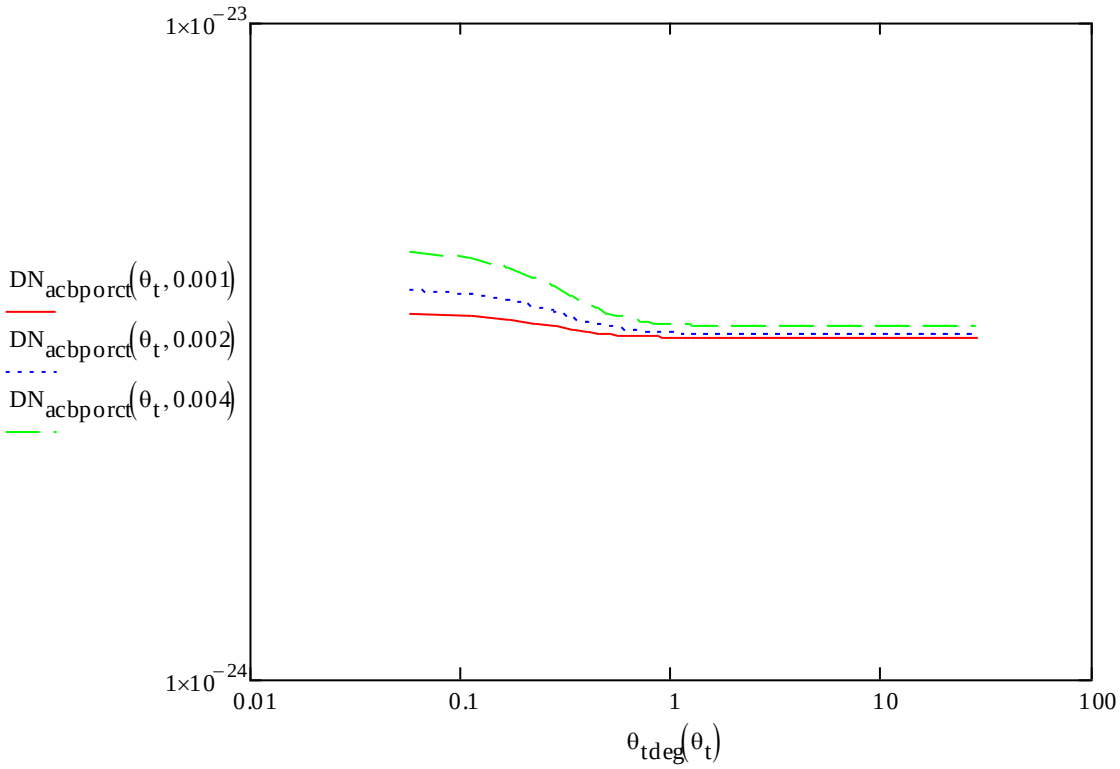

Figure 12: Displacement Noise, Total ACB Scatter, Porcelainized Steel

The glint portion of the displacement noise can be eliminated by tilting the ACB at 1 deg, so that the scattering from the louver surfaces dominates.

3.2.5.2 Oxidized Polished Stainless Steel Scatter Noise

The large angle BRDF of the oxidized stainless steel is approximately two times larger than that of porcelainized steel.

$$BRDF_{ACBoxy}\left(2.57\cdot\frac{\pi}{180}\right) = 0.081$$

The displacement noise from scattering by the higher BRDF oxidized polished stainless steel is slightly larger than for the porcelainized steel, as shown in the Figure 13. For oxidized polished stainless steel, the scatter from the louver surface is larger than the glint from the edges and dominates the scatter at all tilt angles.

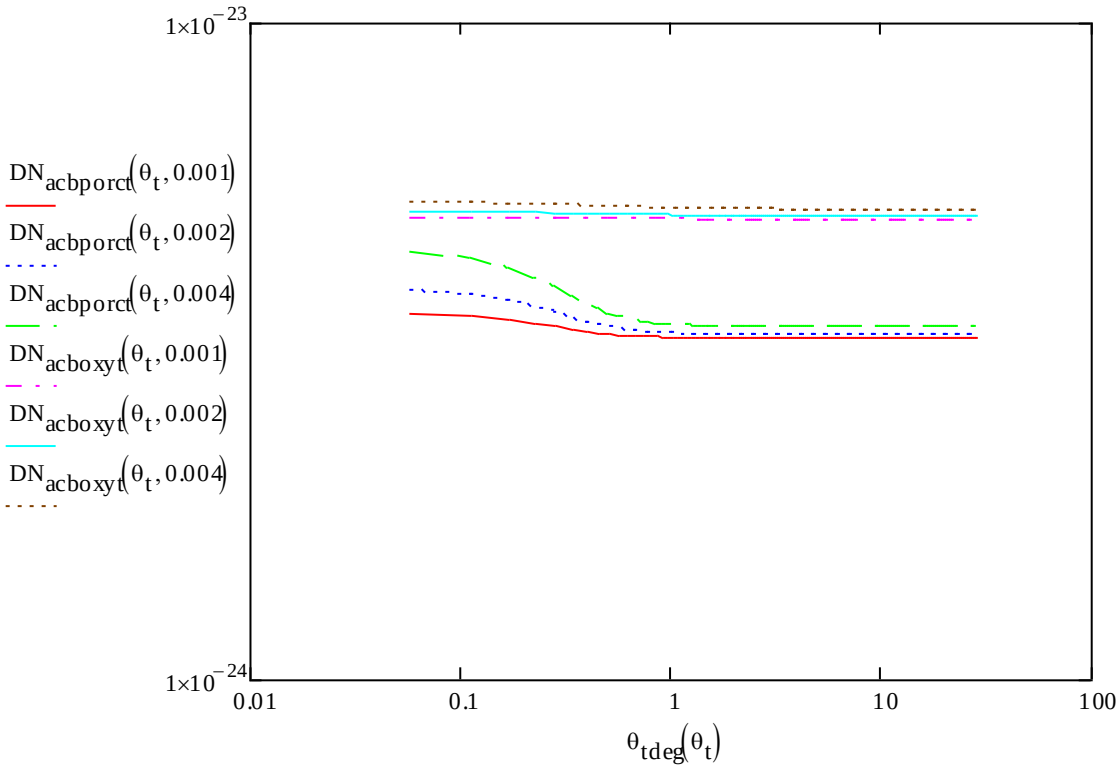

Figure 13: Displacement Noise, Total ACB Scatter, Porcelainized Steel and Oxidized Polished Stainless Steel